Publié dans Inorganica Chimica Acta 359, issue 6, 1929-1938, 2006
qui doit être utilisé pour toute référence à ce travail

Synthesis and structural analysis of palladium biscarbene complexes derived from bisimidazolium ligand precursors

Marion Heckenroth [a], Antonia Neels [b], Helen Stoeckli-Evans [b], Martin Albrecht [a,*]

[a] *Chemistry Department, Laboratory of Organometallic Synthesis, University of Fribourg, Ch. du Musée 9, CH-1700 Fribourg, Switzerland*
[b] *Institut de Chimie, Laboratoire de Cristallographie, Université de Neuchâtel, Av. de Bellevaux 51, C.P. 2, CH-2007 Neuchâtel, Switzerland*

Dedicated to Gerard van Koten with deep appreciation for his outstanding contribution to the organometallic chemistry of late transition metals.

Abstract

The palladation of potentially chelating bisimidazolium ligand precursors with palladium acetate gives bridging bimetallic, chelating monometallic, and homoleptic tetracarbene complexes. The coordination mode of the biscarbene ligand has been identified by spectroscopic analysis and crystallographic characterization of representative complexes, including the first example of a biscarbene A-frame structure. Substantial concentrations of free acetate favor the formation of tetracarbene over biscarbene palladium complexes, while in the absence of a base, the concentration of reactants influences the selectivity for bridging bimetallic versus chelating monometallic species. Preliminary kinetic and mechanistic studies indicate that chelating biscarbene palladium acetate complexes are intermediates in the formation of the homoleptic tetracarbene complexes. Probably due to the high *trans* effect of the biscarbene ligand, such complexes are more efficient palladating agents for bisimidazolium salts than palladium acetate.

Keywords: Palladium; *N*-heterocyclic carbenes; Chelation; Heteroleptic complexes; Mechanism of metallation

1. Introduction

Ionic liquids, in particular those derived from imidazolium ions such as [bmim][PF_6], have received considerable interest as robust and versatile solvents for organometallic reactions [1]. However, many of these imidazolium-based solvents suffer from a low resistance towards bases [2], which often hampers their application as inert solvents. Base-induced deprotonation leads to *N*-heterocyclic carbenes which may ligate the metal center and hence change its activity. While this reactivity pattern represents a serious drawback in the use of ionic liquids as solvents for metal-catalyzed reactions, it also stimulated the exploitation of such carbenes as novel class of ligands in transition metal chemistry [3]. In fact, the selective abstraction of the imidazolium-H(2) proton followed by metallation, either in situ or after isolation of the free carbene, probably constitutes the procedure that is most widely applied for the preparation of metal carbene complexes [3–5].

Despite of the relevance of this methodology, little is known about the mechanistic details of the metallation process, which becomes particularly important when using polydentate ligand systems. An early investigation indicates that the cyclopalladation of a bisimidazolium ligand precursor is, in the absence of a base, a stepwise process involving sequential palladium–carbene bond formation [6]. In addition, the isolation of various thermally stable bimetallic complexes indicates that the metal–carbene bond is kinetically stable [7]. Unlike phosphines or other neutral donors, carbenes do not transiently dissociate from and reassociate to the metal center, e.g., during a catalytic cycle [8]. This behavior also accounts for the thermal stability

* Corresponding author. Tel.: +41 26 300 8786; fax: +41 26 300 9738.
E-mail addresses: helen.stoeckli-evans@unine.ch (H. Stoeckli-Evans), martin.albrecht@unifr.ch (M. Albrecht).

of bimetallic complexes containing bridging carbene ligands derived from bisimidazolium precursors. The kinetically rigid bonding of carbenes prevents the transformation of such bimetallic complexes into thermodynamically favored chelates. Chelation of biscarbenes thus requires specific conditions for the deprotonation and subsequent metallation [9].

We now report the palladation of potentially chelating bisimidazolium precursors under different reaction conditions, thus affording carbene complexes with various coordination modes. Mechanistic and kinetic investigations in the presence and in the absence of additional base provide further insight into factors that determine the product selectivity, thus completing the results from previous studies [6]. Moreover, we describe the structural features of the formed complexes, including the crystallographic characterization of an unusual bimetallic A-frame carbene complex. Notably, this structural motif is only accessible when using potentially chelating biscarbene ligand precursors.

2. Experimental

2.1. General

The ligand precursor **1a** [10] and **1b** [9d] and the palladium complex **2a** [11] were prepared according to the literature procedures, all other reagents are commercially available and are used as received. All NMR spectra were recorded at 25 °C on Bruker Avance 360 and Bruker Avance DRX 500 spectrometers at 360 or 500 MHz (^{1}H NMR) and 90 or 125 MHz (^{13}C NMR), respectively, and referenced to $SiMe_4$ (δ in ppm). Mass spectra were measured by electrospray ionization (ESI-MS, positive mode) in MeCN on a Bruker 4.7 T BioAPEX II instrument. Elemental analyses were performed by the Microanalytical Laboratory of Ilse Beetz, Kronach (Germany).

2.1.1. *[PdI$_2$(biscarbene$^{Pr}_2$)] (**2b**)*

A DMSO solution (10 mL) of **1b** (0.97 g, 2 mmol) and [Pd(OAc)$_2$] (0.45 g, 2 mmol) was stirred at 50 °C for 3 h and then at 110 °C for 2 h. After cooling, the solution was poured into CH_2Cl_2 (20 mL), and Et_2O was added (80 mL). The yellow precipitate was isolated and purified by suspending the product in CH_2Cl_2 and precipitation with Et_2O (3×). After drying in vacuo, a yellow solid was obtained. Crystals suitable for a crystal structure determination were obtained by slow diffusion of Et_2O into a DMSO solution. Yield: 0.91 g, 77%. ^{1}H NMR (500 MHz; DMSO-d_6): δ 7.63 (s, 2H, H_{imi}); 7.53 (s, 2H, H_{imi}); 6.25 (s, 2H, NCH_2N); 5.37 (br, 2H, $CHMe_2$); 1.43 (d, $^3J_{HH} = 6.6$ Hz, 6H, $C(CH_3)Me$); 1.22 (d, $^3J_{HH} = 6.6$ Hz, 6H, $CMe(CH_3)$). $^{13}C\{^1H\}$ NMR (125 MHz; DMSO-d_6): δ 162.46 ($C_{carbene}$); 122.33 (C_{imi}); 118.14 (C_{imi}); 62.64 (NCH_2N); 53.17 ($CHMe_2$); 23.60 ($C(CH_3)Me$), 21.00 ($CMe(CH_3)$). *m/z* (100%): 506.01 (M−I+MeCN). Elem. *Anal*. Calc. for $C_{13}H_{20}I_2N_4Pd$ (591.88): C, 26.35; H, 3.40; N, 9.46. Found: C, 26.30; H, 3.32; N, 9.48%.

2.1.2. *[PdBr$_2$(biscarbene$^{Pr}_2$)] (**2c**)*

Method A: To a solution of **4** (0.60 g, 1.0 mmol) in MeCN (20 mL) was added NBu_4Br (0.97 g, 3.0 mmol) dissolved in MeCN (10 mL). Immediately, a precipitate formed, which was collected by filtration, suspended in CH_2Cl_2 and precipitated by addition of Et_2O. After drying in vacuo, **2c** was obtained as a white solid (0.43 g, 86%).

Method B: A solution of **2b** (0.60 g, 1.0 mmol) in DMSO (5 mL) was stirred in the presence of BnBr (1.0 mL, 8.4 mmol) for 16 h. Subsequent addition of CH_2Cl_2 (20 mL) followed by Et_2O (80 mL) afforded a yellow precipitate, which was washed 3× by suspension in CH_2Cl_2 and precipitation with Et_2O and then dried in vacuo. Analytically pure **2c** was obtained by recrystallization from CH_2Cl_2/Et_2O.

^{1}H NMR (500 MHz; DMSO-d_6): δ 7.62 (s, 2H, H_{imi}); 7.52 (s, 2H, H_{imi}); 6.26 (s, 2H, NCH_2N); 5.49 (br, 2H, $CHMe_2$); 1.43 (d, $^3J_{HH} = 6.6$ Hz, 6H, $C(CH_3)Me$); 1.23 (d, $^3J_{HH} = 6.6$ Hz, 6H, $CMe(CH_3)$). $^{13}C\{^1H\}$ NMR (125 MHz; DMSO-d_6): δ 158.44 ($C_{carbene}$); 122.15 (C_{imi}); 118.10 (C_{imi}); 62.47 (NCH_2N); 52.32 ($CHMe_2$); 23.69 ($C(CH_3)Me$), 21.53 ($CMe(CH_3)$). *m/z* (100%): 419.0 (M–Br). Elem. *Anal*. Calc. for $C_{13}H_{20}Br_2N_4Pd$ (498.55): C, 31.32; H, 4.04; Pd, 21.35. Found: C, 31.16; H, 4.00; Pd, 21.32%.

2.1.3. *[μ-I{PdI(biscarbene$^{Me}_2$)}$_2$]I (**3**)*

A procedure identical to the one described for the preparation of **2a** was used, starting from **1a** (0.86 g, 2 mmol) and [Pd(OAc)$_2$] (0.45 g, 2 mmol). After drying in vacuo, an orange solid was obtained (0.98 g, 95%). NMR analysis revealed a mixture of two compounds in approximately 2:1 ratio. The analytical data of the major product are identical to those of **2a**. Fractional crystallization from DMSO/Et_2O separated the two products and gave crystals of **3** that were suitable for a structure determination.

^{1}H NMR (360 MHz; DMSO-d_6): δ 7.76 (s, 2H, H_{imi}), 7.44 (s, 2H, H_{imi}), 6.77 (lowfield part of AB, $^2J_{HH} = 12.9$ Hz, 2H, NCH*H*N), 6.50 (highfield part of AB, $^2J_{HH} = 12.9$ Hz, 2H, NC*H*HN), 3.36 (s, 6H, NCH_3). $^{13}C\{^1H\}$ NMR (125 MHz; DMSO-d_6): δ 169.52 ($C_{carbene}$); 123.07 (C_{imi}); 122.38 (C_{imi}); 62.73 (NCH_2N); 37.03 (NCH_3). *m/z* (100%): 946.73 (M−I).

2.1.4. *[Pd(biscarbene$^{Pr}_2$)(MeCN)$_2$](BF$_4$)$_2$ (**4**)*

An acetonitrile suspension (8 mL) of **2b** (0.60 g, 1.0 mmol) and $AgBF_4$ (0.41 g, 2.1 mmol) was stirred at RT overnight in the absence of light. The suspension was then filtered through Celite and the acetonitrile removed in vacuo to give an off-white solid (0.56 g, 94%). Analytically pure **4** was obtained by recrystallization from DMSO and Et_2O. ^{1}H NMR (360 MHz; DMSO-d_6): δ 7.74 (s, 2H, H_{imi}); 7.69 (s, 2H, H_{imi}); 6.55 (lowfield part of AB, $^2J_{HH} = 12.0$ Hz, 2H, NCH*H*N), 6.31 (highfield part of AB, $^2J_{HH} = 12.0$ Hz, 2H, NC*H*HN); 4.86 (sept, $^3J_{HH} = 6.6$ Hz, 2H, $CHMe_2$); 2.06 (s, 6H, NCMe); 1.49 (d, $^3J_{HH} = 6.6$ Hz, 6H, $C(CH_3)Me$); 1.33 (d, $^3J_{HH} = 6.6$ Hz,

6H, CMe(CH_3)). $^{13}C\{^1H\}$ NMR (125 MHz; DMSO-d_6): δ 144.98 ($C_{carbene}$); 123.99 (C_{imi}); 119.08 (C_{imi}); 118.08 (Me*C*N); 62.16 (NCH_2N); 51.89 ($CHMe_2$); 24.04 (C(*C*H_3)Me), 21.78 (CMe(CH_3)); 1.14 (*C*H_3CN). Elem. *Anal.* Calc. for $C_{17}H_{26}B_2F_8N_6Pd \times H_2O$ (612.47): C, 33.34; H, 4.61; N, 13.72. Found: C, 33.04; H, 4.41; N, 13.50%.

2.1.5. *[Pd(biscarbeneMe$_2$)$_2$]I$_2$ (**6a**)*

A DMSO solution (10 mL) of **1a** (0.86 g, 2 mmol) and NEt_3 (0.7 mL, 5 mmol) was stirred at RT for 30 min. After addition of $[Pd(OAc)_2]$ (0.22 g, 1 mmol), the reaction mixture was stirred at RT for 3 h, then at 50 °C for 18 h and finally at 150 °C for 1 h. After cooling, the solution was poured into CH_2Cl_2 (20 mL) and Et_2O was added (80 mL). The off-white precipitate was isolated and purified by suspending the product in CH_2Cl_2 and precipitation with Et_2O (3×). After drying in vacuo, an off-white solid was obtained (0.43 g, 60%). Crystals suitable for crystal structure determination were obtained by slow diffusion of Et_2O into a DMSO solution. The analytical data are identical to those reported previously [12,13].

2.1.6. *[Pd(biscarbenePr$_2$)$_2$]I$_2$ (**6b**)*

This complex was prepared following the procedure described for **6a**, starting from **1b** (0.97 g, 2 mmol), NEt_3 (0.7 mL, 5 mmol) and $[Pd(OAc)_2]$ (0.23 g, 1 mmol). This afforded **6b** as an off-white solid (0.60 g, 73%). Recrystallization from DMSO and Et_2O gave crystals suitable for a structure determination.

^1H NMR (360 MHz; DMSO-d_6): δ 7.82 (s, 2H, H_{imi}); 7.53 (s, 2H, H_{imi}); 6.62 (lowfield part of AB, $^2J_{HH}$ = 13.5 Hz, 2H, NCH*H*N); 6.51 (highfield part of AB, ^2J = 13.5 Hz, 2H, NC*H*HN); 3.89 (sept, $^3J_{HH}$ = 6.6 Hz, 2H, $CHMe_2$); 1.27 (d, $^3J_{HH}$ = 6.6 Hz, 6H, C(CH_3)Me); 1.16 (d, $^3J_{HH}$ = 6.6 Hz, 6H, CMe(CH_3)). $^{13}C\{^1H\}$ NMR (125 MHz; DMSO-d_6): δ 169.31 ($C_{carbene}$); 123.27 (C_{imi}); 118.54 (C_{imi}); 63.38 (NCH_2N); 52.64 ($CHMe_2$); 25.22 (C(CH_3)Me); 20.37 (CMe(CH_3)). *m/z* (100%): 697.15 (M−I). Elem. *Anal.* Calc. for $C_{26}H_{40}I_2N_8Pd \times 3DMSO$ (1058.09): C, 36.28; H, 5.52; N, 10.05. Found: C, 36.50; H, 5.34; N, 10.44%.

2.2. Structure determination and refinement of **2b**, **2c**, **3**, **6a**, and **6b**

Crystals were obtained as described in Section 2. Data were collected on a Stoe Mark II-Image Plate Diffraction System [14] using Mo Kα graphite monochromated radiation (λ = 0.71073 Å). The structures were solved by direct methods using SHELXS-97 [15] and the refinement and all further calculations were carried out using SHELXL-97 [16]. The H-atoms were included in calculated positions and treated as riding atoms using SHELXL default parameters. The non-H atoms were refined anisotropically using weighted full-matrix least-squares on F^2. Semi-empirical absorption corrections were applied (MULABS [17]). The crystal of **2b** was twined and the TWIN integration method included in the Stoe software [14] was used. More than 30% of the reflections were overlapped and hence removed from the final

Table 1
Crystallographic data for **2b**, **2c**, **3**, **6a**, and **6b**

	2b	**2c**	**3**	**6a**	**6b**
Color, shape	yellow rod	yellow rod	orange plate	yellow rod	colorless rod
Crystal size (mm)	0.45 × 0.23 × 0.23	0.45 × 0.20 × 0.20	0.30 × 0.30 × 0.10	0.40 × 0.30 × 0.20	0.50 × 0.45 × 0.40
Empirical formula	$C_{15}H_{26}I_2N_4OPdS$	$C_{14}H_{22}Br_2Cl_2N_4Pd$	$C_{22}H_{36}I_4N_8O_2Pd_2S_2$	$C_{20}H_{30}I_2N_8OPdS$	$C_{32}H_{57}I_2N_8O_{2.5}PdS_2$
Formula weight	670.66	583.48	1229.11	790.78	1018.18
T (K)	173	293	173	173	173
Crystal system	monoclinic	orthorhombic	orthorhombic	trigonal	triclinic
Space group	$P2_1$ (No. 4)	*Pnma* (No. 62)	*Cmcm* (No. 63)	$R\bar{3}$ (No. 148)	$P\bar{1}$ (No. 2)
Unit cell dimensions					
a (Å)	7.5005(5)	13.8392(8)	11.7827(15)	20.5799(8)	11.2758(9)
b (Å)	15.5606(13)	15.7531(10)	13.5635(11)	20.5799(8)	12.3994(10)
c (Å)	9.6755(6)	9.6504(8)	22.479(2)	17.8979(7)	16.2138(13)
α (°)	90	90	90	90	103.545(6)
β (°)	106.012(7)	90	90	90	103.174(6)
γ (°)	90	90	90	120	99.046(6)
V (Å^3)	1085.44(13)	2103.9(3)	3592.6(6)	6564.8(4)	2092.1(3)
Z	2	4	4	9	2
D_{calc} (g cm^{-3})	2.052	1.842	2.272	1.800	1.616
μ (Mo Kα) (mm^{-1})	3.805	4.937	4.587	2.850	2.058
Reflections total, unique	5243, 2662	32835, 2953	18301, 1737	27251, 3960	26688, 11221
R_{int}	0.0301	0.0850	0.0754	0.0376	0.0376
Transmission factors min., max.	0.451, 0.756	0.246, 0.491	0.303, 0.446	0.387, 0.522	0.453, 0.683
Parameters, restraints	200, 1	94, 0	104, 0	174, 5	437, 0
R_1,[a] wR_2[b]	0.0254, 0.0645	0.0349, 0.0791	0.0362, 0.0860	0.032, 0.0866	0.0313, 0.0759
S	1.037	1.049	0.955	1.046	1.036
Residual density min., max. (e Å^{-3})	−0.741, 0.981	−1.162, 0.502	−2.073, 0.886	−0.957, 1.190	−1.075, 3.293

[a] $R_1 = \sum||F_O| - |F_C||/\sum|F_O|$ for all $I > 2\sigma(I)$.
[b] $wR_2 = [\sum w(F_O^2 - F_C^2)^2 / \sum(w(F_O^4))]^{1/2}$.

data set. A check (SQUEEZE [17]) of the unit cell of **2c** indicated a 479 Å^3 solvent-accessible area containing ca. 185e. Therefore, four CH_2Cl_2 molecules (4×48e) were included in the unit cell for all further calculations. All calculations and graphical illustrations were performed with the PLATON03 [17] package. Crystal data are given in Table 1.

3. Results and discussion

3.1. Chelation versus bridging coordination of biscarbenes

Palladium complexes containing chelating bis(imidazolylidene) *N*-heterocyclic carbene ligands are usually prepared by heating the corresponding imidazolium ligand precursor in the presence of a metal salt containing a Lewis-basic ligand such as $[Pd(OAc)_2]$ [18]. When using these reaction conditions with the bisimidazolium salt **1a**, we indeed observed the formation of the known [11] **2a** as the major product (62%, Scheme 1). As a minor product, however, the bridged bimetallic complex **3** was detected in 33% yield (Scheme 1). Qualitatively, the ^{1}H NMR spectroscopic data of **3** are very similar to those of **2a** except for an AB doublet located at δ_H 6.73 and 6.50 (DMSO-d_6 solution) attributed to the bridging methylene group. The inequivalence of these CH_2 protons suggests a fixed bonding mode of the biscarbene and restricted rotation about the Pd–$C_{carbene}$ bonds, which is not the case in **2a** (singlet at δ_H 6.28) [11]. Mass spectrometric analysis using electron spray ionization (ESI) provides a signal at 946.73 as the most intense fragment. This corresponds to the $[Pd_2(biscarbene)_2I_3]^+$ cation and hence supports a dimetallic species. Moreover, the observed isotopic pattern is in excellent correlation with a dipalladium ion containing three iodine residues. While the above information does not allow to distinguish **3** from a face to face bimetallic structure

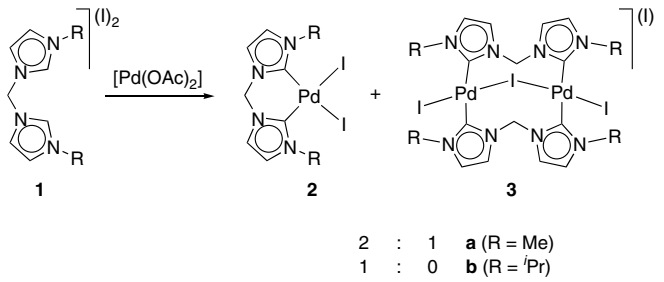

Scheme 1.

comprising two neutral PdI_2 moieties, an X-ray structure determination was conclusive. Crystals suitable for a structure determination were obtained by slow diffusion of Et_2O into a DMSO-solution of **3**. Complex **3** crystallizes with 2 moleq. DMSO in the centrosymmetric orthorhombic space group C*mcm*. The cationic residue of **3** shows an A-frame structure [19] comprising a monocationic palladium dimer bridged by an iodide ligand (Fig. 1(a)). While A-frames are typically encountered with diphosphine ligands, complex **3** represents to the best of our knowledge the first characterized biscarbene A-frame. The high symmetry of the molecular structure of **3** (Fig. 1(b)) is best reflected by the fact that the iodine atom I2 is located on a crystallographic symmetry plane and simultaneously on a C_2 rotation axis. The palladium centers are crystallographically equivalent and are located in a slightly distorted square-plane (Table 2). Due to the bridging coordination mode, the carbene ligand adopts an orientation that is virtually perpendicular to the palladium square-plane, the torsion angle I1–Pd1–C1–N2 being 86.7(5)°. As may be expected from such a structure, the capping iodide ligands are closer to the metal center (Pd1–I1 is 2.5692(19) Å) than the bridging iodide (Pd–I2 2.6244(9) Å).

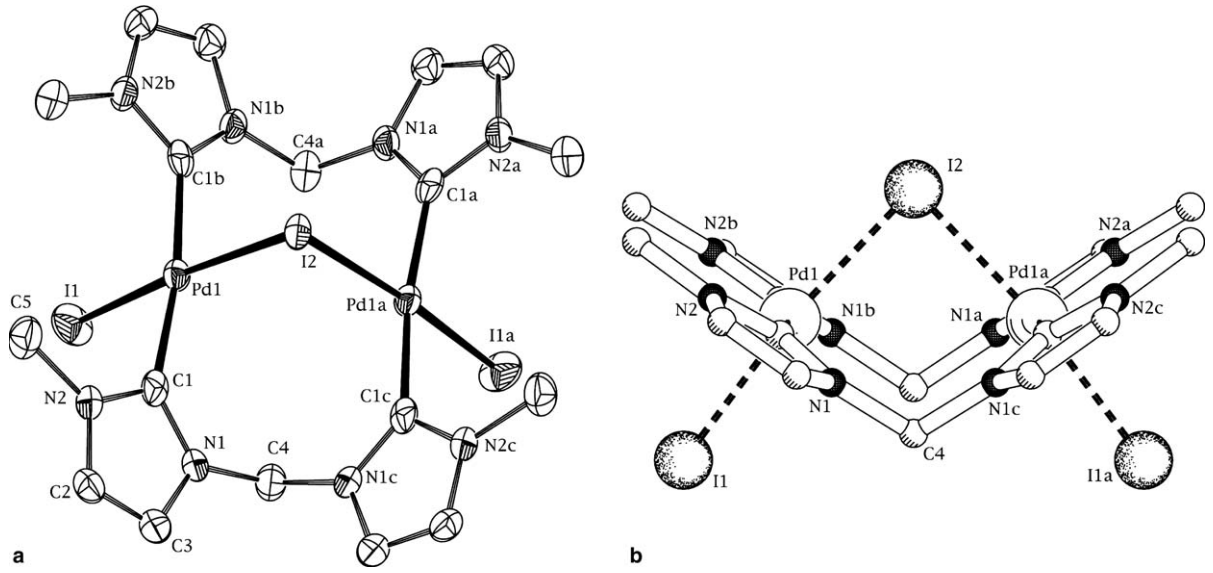

Fig. 1. Molecular structure of **3**. (a) Thermal ellipsoid plot of **3** (50% probability); the non-coordinating iodide, the co-crystallized solvent molecules and the hydrogen atoms have been omitted for clarity. (b) Perspective view of **3**, emphasizing the highly symmetric A-frame structure.

Table 2
Structural data of complex **3**

Bond lengths (Å)		Bond angles (°)	
Pd1–C1	2.017(7)	C1–Pd1–C1b	171.8(4)
Pd1–I1	2.5692(10)	C1–Pd1–I1	88.19(17)
Pd1–I2	2.6244(9)	C1–Pd1–I2	92.21(7)
C1–N1	1.353(9)	I1–Pd1–I2	173.51(4)
C1–N2	1.357(9)	Pd1–I2–Pd1a	86.64(4)
C2–C3	1.335(10)	N1–C4–N1c	111.6(8)

The formation of Pd–$C_{carbene}$ bonds from imidazolium salts and $[Pd(OAc)_2]$ is generally assumed to pass through a six-membered transition state, in which an acetate ion is coordinated to the acidic proton and simultaneously to the palladium center through one oxygen each (**A**, Scheme 2). Release of HOAc will then give a palladium carbene complex such as **B** [6] containing an acetate ion as spectator ligand. Subsequent cyclometallation is expected to yield **2**, presumably promoted by the metal-bound acetate via formation of another six-membered transition state. Structure **C** may represent a potential arrangement for this transition state. This process is expected to be favored by the constantly high palladium concentration around the imidazolium site of the monocarbene complex **B**. In addition, intermediate **B** constitutes a pre-organized structure, as the monocarbene is covalently linked to the imidazolium fragment, thus properly arranging the Pd with respect to the imidazolium C–H bond. The observed formation of **3**, however, implies that the second imidazolium C–H bond is not activated by cyclometallation but via another independent palladium precursor, viz. either a monocarbene **B** or $[Pd(OAc)_2]$ (cf. intermediate **D** in Scheme 2 with L^1 = monocarbene, L^2 = OAc and L^1, L^2 = η^2-OAc, respectively). Such an intermolecular metallation might be competitive with intramolecular palladation by the [Pd(OAc)(carbene)X] fragment due to a relatively high concentration of the metal precursor. However, measurements at different concentrations (0.05–1.0 M) showed a preference for **3** under dilute reaction conditions. According to ^{1}H NMR integration of the methylene protons, the **2b**:**3** ratio changes from 2.6:1 at 1.0 M to about 0.4:1 at 0.05 M. At this point, we do not have any explanation for this apparently contradictory influence of the concentration of reactants on the product distribution.

Palladation of the *iso*-propyl substituted bisimidazolium salt **1b** under analogous reaction conditions gives the monometallic biscarbene palladium complex **2b** as the exclusive product in high yields (Scheme 1). Analyses of the crude reaction mixture by NMR spectroscopy before crystallization did not indicate any traces of a bridged dipalladium species similar to that of **3**. Chelation of the biscarbene can be deduced from the ^{1}H NMR spectrum, which shows a singlet resonance at δ_H 6.25 for the methylene protons bridging the two carbene units. The ESI spectrum shows a maximum intensity at 506 with the correct isotopic pattern for the $[M-I+MeCN]^+$ fragment of **2b**. This is in agreement with the proposed monometallic structure rather than a bridged dimetallic species. Notably, the spectrum also shows small intensities for di- and oligomeric fragments. Since the sample was a single compound according to its ^{1}H NMR spectrum, we presume that such higher species are only formed upon ionization within the mass spectrometer and that they are not present prior to injection.

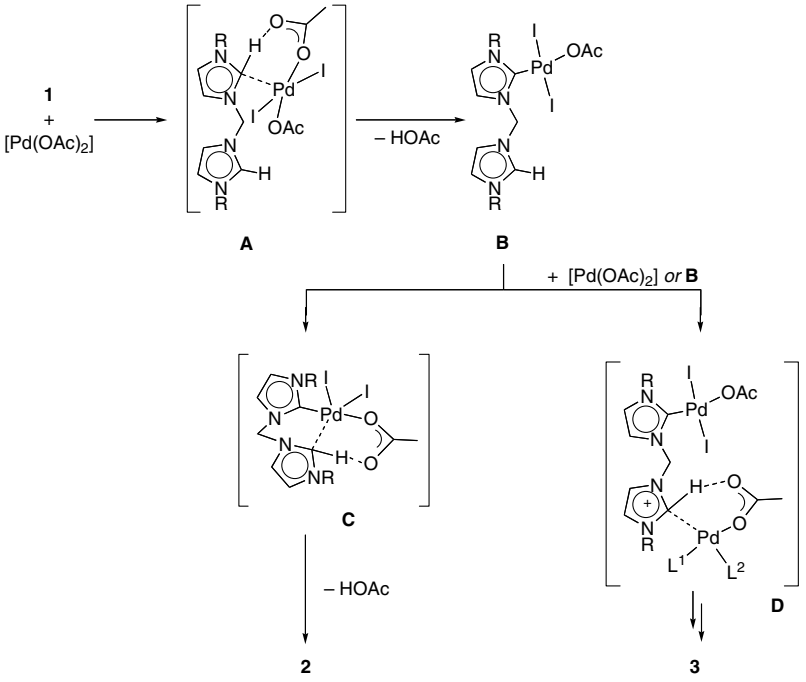

Scheme 2.

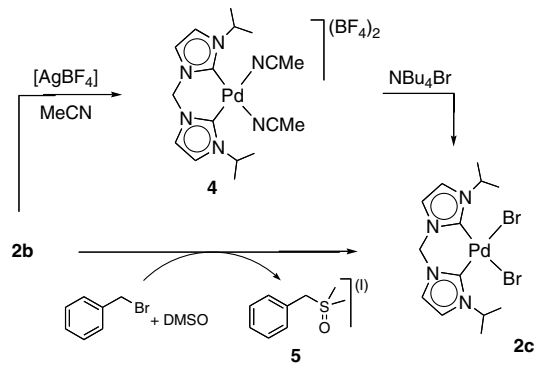

Scheme 3.

Substitution of the metal-bound iodides in **2b** has been realized by two different methods (Scheme 3). Silver-mediated iodide abstraction followed by addition of excess NBu_4Br corresponds to the standard method to form **2c** [20]. This route involves the formation of the halide-free complex **4** as an intermediate that can be isolated and purified from any residual iodide. The most sensitive nucleus for this halide exchange is, of course, the metal-bound carbon, which is displaced from δ_C 162.5 to δ_C 158.4 upon exchange of the two metal-bound iodides with bromides. The resonance for the proton attached to the tertiary isopropyl carbon provides another diagnostic probe for the metal-bound halide X, as it moves from δ_H 5.37 (X = I, **2b**) to δ_H 5.49 (X = Br, **2c**). In either complex, the septett is unresolved and appears as a broad signal ($w_{1/2} = 50$ Hz at 500 MHz and RT). The observed chemical shift difference may be due to the different *trans* influence of the metal-bound halide, which would increase the acidity of the pseudo-benzylic protons in **2c** relative to **2b**. However, the bridging methylene group does not undergo a comparable shift upon halide exchange. A more plausible explanation is therefore offered by intramolecular hydrogen bonding of these pseudo-benzylic protons to the metal-bound halide. Indeed, such H-bonds should be stronger with an accepting bromide than with iodide.

An alternative route towards the bromide complex **2c** consists of the reaction of **2b** in DMSO in the presence of alkyl bromides such as EtBr or BnBr (Scheme 3). A plausible mechanism for this less usual procedure comprises the oxidative addition of the alkyl bromide to the palladium center, followed by a reductive elimination of the alkyl ioodide or, more probably, of its sulfonium salt. The strong σ-donation of the biscarbene ligand in **2b** is expected to favorably support palladium oxidation. While we were not able to sufficiently stabilize the proposed Pd^{IV} intermediate for (spectroscopic) characterization, activation of the C–Br bond has been confirmed by the detection of the sulfonium salt **5** (Scheme 3) [21].[1] Upon heating, **5** decomposed to SMe_2 and benzaldehyde, as confirmed by ^{1}H NMR spectroscopy. While the DMSO-mediated oxidation of benzyl halides is known to proceed even in the absence of a metal catalyst [22], the formation of BnI or **5** and **2c** requires, in our case, the activation of the C–Br bond and hence the involvement of **2b**. A comparable reactivity of **2b** with an excess of alkyl bromides is observed in MeCN. This indicates that the formation of the sulfonium intermediate is not essential for the formation of **2c**, though polar solvents facilitate the oxidative RX addition to these biscarbene complexes.

[1] No sulfonium salt has been detected when EtBr was used as a bromide source, probably owing to the reduced cation stabilization of Et compared to Bn, leading to rapid decomposition and formation of volatile acetaldehyde.

3.2. Solid state structures of *2b* and *2c*

Single crystal structure determinations were carried out for **2b** and **2c** (Figs. 2(a) and (b), respectively). The Pd–C bond lengths in the iodide complex **2b** are 1.983(6) and 2.000(7) Å and compare well with related palladium complexes containing methyl and *t*-butyl wingtips on the biscarbene (Table 3) [6,11]. Furthermore, the angle between the two carbene ligands C–Pd–C 83.3(2)° is identical within esd's in all these biscarbene palladium iodides. Apparently, the biscarbene bite angle to a PdI_2 fragment remains virtually unaffected by steric modification of the wingtip groups. The structure of the bromide analog **2c** reveals two carbene moieties that are also crystallographically symmetry-related. The Pd–C bond (1.972(3) Å) is slightly shorter than in the corresponding iodide complex **2b**, thus reflecting the lower *trans* influence of bromide versus iodide. In addition, a weak intramolecular hydrogen bond between the bromide and the pseudo-benzylic proton is observed with H5···Br1 2.79 Å and C5···Br1 3.556(4) Å. The hydrogen bond angle C5–H5···Br1 is 135° and hence rather acute [23]. This structural motif apparently prevails also in solution, albeit to a weaker extent (cf. NMR discussion). No similar interaction is seen in the iodide complex, maybe due to the longer palladium–halide bond distance and hence a less favorable donor–acceptor alignment.

3.3. Tetracarbene palladium complexes

The presence of a base has a pronounced effect on the metallation of these bisimidazolium salts. Heating of the bisimidazolium salt **1** and $[Pd(OAc)_2]$ with NEt_3 (2 moleq.) according to the protocol applied for the synthesis of **2** gave the ionic tetracarbene palladium complex **6** in good yields (Scheme 4). This reaction scheme represents a further simplification of the preparation of homoleptic carbene complexes. Initially, **6a** was prepared in low yields from **1a** with BuLi as the base [12], later a two-step procedure was reported using NaOAc [13]. Both complexes **6a** and **6b** appeared to be virtually insoluble in organic solvents such as CH_2Cl_2 or $CHCl_3$, though very soluble in polar solvents like DMSO. The ^{1}H NMR spectra of **6** show distinct differences when compared to the neutral biscarbene complexes **2**. The well-resolved AB

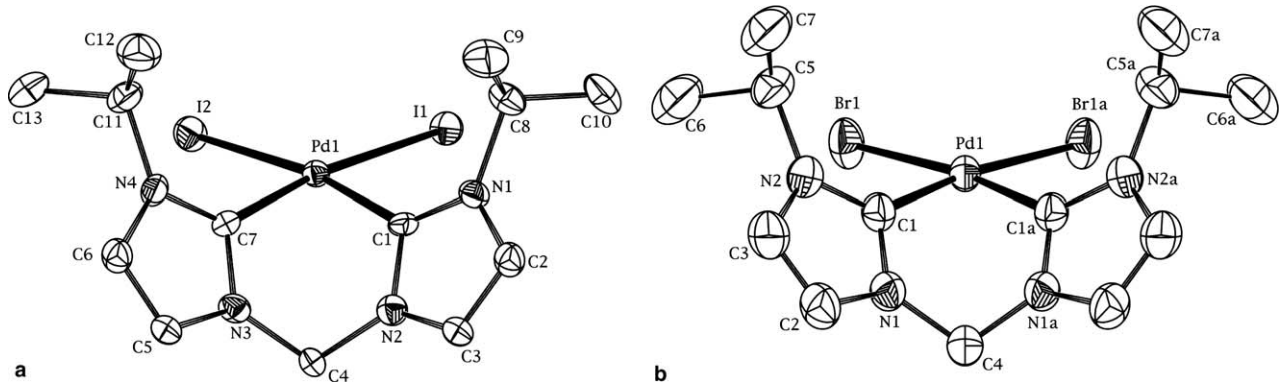

Fig. 2. Thermal ellipsoid plots (50% probability) of **2b** (a) and **2c** (b); the co-crystallized solvent molecules and the hydrogen atoms have been omitted for clarity.

Table 3
Bond lengths (Å) and angles (°) in biscarbene complexes **2**

	2a (X = I)[a,b]	**2b** (X = I)	**2c** (X = Br)[a]	**2d** (X = I)[a,c]
Bond lengths				
Pd1–C1	1.989(8)	1.983(6)	1.972(3)	2.004(3)
Pd1–C7	1.988(7)	2.000(7)	1.972(3)	2.004(3)
Pd1–X1	2.6450(9)	2.6580(5)	2.4876(4)	2.6694(3)
Pd1–X2	2.6573(8)	2.6552(6)	2.4876(4)	2.6694(3)
Bond angles				
C1–Pd1–C7	83.2(3)	83.3(2)	83.64(18)	83.3(2)
C1–Pd1–X1	92.0(2)	91.34(16)	91.56(9)	91.65(7)
C1–Pd1– X2	170.0(2)	170.58(18)	172.77(9)	167.27(8)
C7–Pd1– X1	172.8(2)	172.44(17)	172.77(9)	167.27(8)
C7–Pd1– X2	90.9(2)	92.14(18)	91.56(9)	91.65(7)
X1–Pd1– X2	93.16(3)	92.331(18)	92.69(2)	90.79(1)

[a] Atom labeling adapted to labeling scheme in Fig. 2(a).
[b] From [11].
[c] R = *t*Bu (Scheme 1) from [6].

doublets around 6.6 and 6.3 ppm were noted previously and associated with a rigid boat-type conformation of the six-membered metallacycle. In the corresponding biscarbene complexes, the observed singlet resonance indicates a higher degree of conformational flexibility. Furthermore, coordination of a second biscarbene ligand induces a significant high-field shift of the wingtip α-hydrogens . The shift is more pronounced in the isopropyl substituted complex **6b** (δ_H 3.85, $\Delta\delta = 1.52$ ppm) than in the methyl analog **6a** (δ_H 3.38, $\Delta\delta = 0.47$ ppm) and may reflect the increasing steric congestion around the palladium center upon coordination of a second biscarbene ligand.

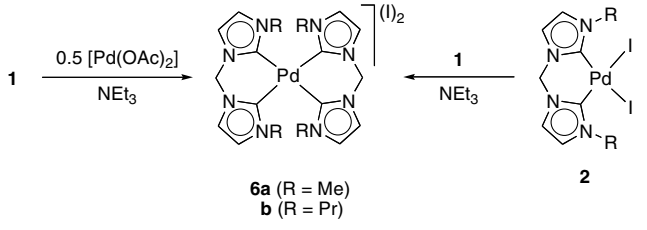

Scheme 4.

The steric effects of the substituents have been investigated in more detail by crystallographic analyses of these tetracarbene complexes. For this purpose, the structural data of **6a** have been redetermined [12] from crystals obtained from DMSO/Et_2O solution. The unit cell contains two disordered molecules of DMSO and consequently differs considerably from the structure **6a'** previously reported by Fehlhammer et al., which contains a cocrystallized molecule of H_2O. The unit cell of **6b** reveals two crystallographically independent palladium cations with virtually identical bond lengths and angles. The geometries around the palladium center are highly similar in **6a** and **6b** (Figs. 3(a) and (b), respectively, Table 4), but remarkably not in **6a'**. For example, the Pd–C bond lengths are consistently between 2.025(2) and 2.037(2) Å and hence slightly longer than in the analoguous biscarbene complex **2**, yet shorter than in **6a'** (Pd–C up to 2.137(5) Å). This relative increase of the bond length can be attributed to the *trans* influence, which is higher for the carbene ligand than for iodide. A significant difference between **6a** and **6b** is noted when comparing the mutual torsion of the carbene heterocycles and the palladium square plane. In **6b** containing bulky isopropyl wingtip groups, the N–C–Pd–C dihedral angles are between 41.6° and 43.6°, while in **6a** containing smaller methyl groups, the cycles are in a mutually more planar arrangement with dihedral angles in the 39.1–39.7° range. A similar conclusion can be drawn from ligand bite angle analysis: the C1–Pd1–C7 angle is significantly smaller in the isopropyl substituted complex **6b** than in **6a**, indicating a steric compression of the biscarbene ligand. The pronounced out-of-plane arrangement with respect to the palladium square plane in the tetracarbene complexes corroborates the results from comparative NMR analyses of **2b** and **6** in solution (vide supra).

3.4. Role of the bases

Metal precursors containing basic acetate or carbonate ligands appear to be particularly useful for the metallation of imidazolium salts [9]. In addition to their potential to form favorable six-membered metallacyclic transition

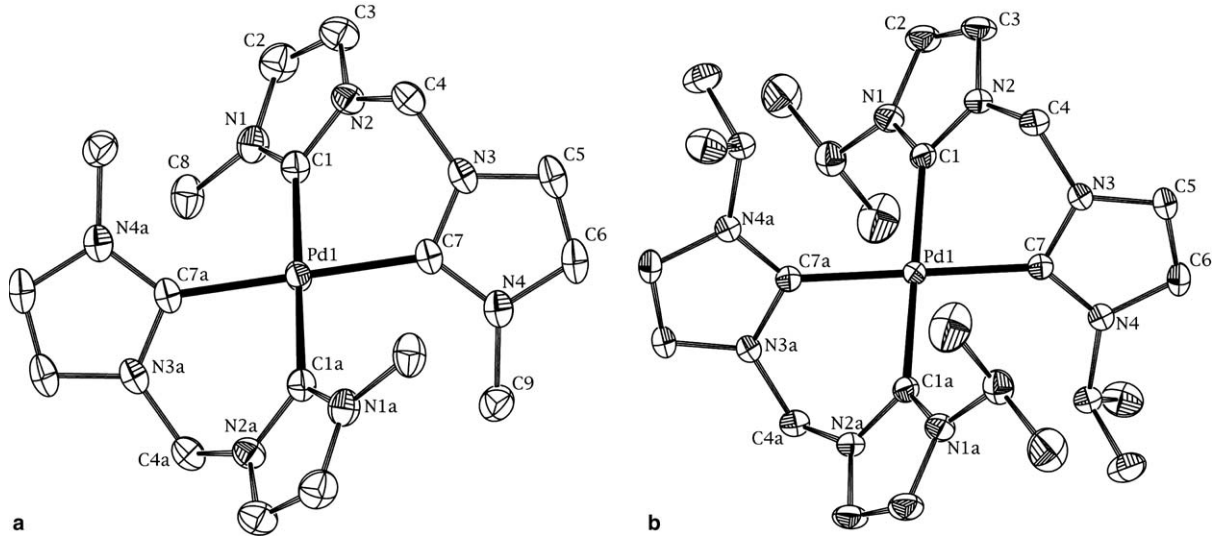

Fig. 3. Molecular structures (50% probability) of the dications **6a** (a) and **6b** (b); the second crystallographically independent cation of **6b**, the co-crystallized solvents, the iodide counterions, and the hydrogen atoms have been omitted for clarity.

Table 4
Bond lengths (Å) and angles (°) in complexes **6a**, **6a**' and **6b**

	6a	**6a**[a,b]	**6b**	**6b**[a,c]
Bond lengths				
Pd1–C1	2.034(3)	2.137(5)	2.037(2)	2.038(2)
Pd1–C7	2.029(3)	2.049(4)	2.025(2)	2.030(2)
C2–C3	1.346(5)	1.324(6)	1.334(4)	1.335(4)
C5–C6	1.346(5)	1.337(9)	1.335(4)	1.335(4)
Bond angles				
C1–Pd1–C7	84.71(12)	81.8(2)	83.46(10)	83.80(9)
C1–Pd1–C7a	95.29(12)	98.2(2)	96.54(10)	96.20(9)
C1–Pd1–C1a	180.0	180.0	180.0	180.0

[a] Atom labeling adapted to labeling scheme in Fig. 3.
[b] From [12] containing co-crystallized H_2O.
[c] Second independent molecule in the unit cell.

states (vide supra), these precursors ensure a permanent bonding of the basic sites and hence avoid an excess of free base in the reaction mixture. The formation of the tetracarbene complexes **6**, however, requires addition of an external base, which has a pronounced influence on the metallation. When using equimolar amounts of the bisimidazolium ligand precursor **1b** and [$Pd(OAc)_2$], i.e., conditions that should favor the formation of **2b**, we observe the formation of the tetracarbene complex **6b** only. This rather selective formation of **6b** under basic conditions may be a direct consequence of the steady concentration of free acetate as ligand and initial C–H bond activator. In the absence of a base, the concentration of free acetate is negligible due to the stoichiometric formation of HOAc, while under basic conditions, the released proton is trapped by NEt_3. Moreover, ion pairing of the ammonium cation with halides might be more tight than with acetate, thus favoring an acetate analog of **2** as an intermediate. Owing to the high *trans* effect of the biscarbene this acetate ligand is significantly more labile in **2** than in [$Pd(OAc)_2$], which results in an increased reactivity of the acetate analog of **2**. Both these effects support the observation that the first (cyclo)metallation of the bisimidazolium ligand is slower than the second one.

Notably, **6** can be obtained from the bisimidazolium precursor **1** either directly (see above) or in a sequential reaction via initial formation of **2** in the absence of an external base, and subsequent reaction of **2** and another equivalent of ligand in the presence of a base such as NaOAc [13] or NEt_3. In order to check whether **2** is an intermediate during the direct formation of **6**, the reaction of [$Pd(OAc)_2$] with 2 moleq. **1b** was performed in DMSO-d_6 at 70 °C and followed by ^{1}H NMR spectroscopy. At these temperatures considerably longer reaction times (>20 h) are required to achieve high yields.

Time-dependent NMR spectroscopy shows the rapid consumption of **1b** at room temperature and concomitant formation of a mixture of products. The major component of the reaction mixture displays a set of NMR signals that is consistent with a monocarbene complex such as **B** (Scheme 2) [6,9d]. The structure is characterized by a desymmetrized resonance pattern featuring two distinct isopropyl groups, and five inequivalent imidazol-bound protons in the aromatic region. The deshielding of one of these protons (δ_H 11.56) is similar to those in **1b**, while the other four protons are located between 7.5 and 8.1 ppm. This intermediate **B** is observed in large concentrations when the reaction is kept at room temperature. Upon warming to 70 °C, the signals due to **B** rapidly disappear, presumably via a transition state similar to that of **C** (Scheme 2). Formation of **2b** and, consecutively, **6b** is indicated by the evolution of the pertinent resonance patterns. No further intermediates have been detected during the **2b** to **6b** transformation, suggesting that the activation of the imidazolium ligand by **2b** constitutes the rate-determining step in this process. This is in

contrast to the first metallation step, in which chelation, i.e., the activation of the second imidazolium residue is rate-determining.

4. Conclusions

Palladation of bisimidazolium salts gives palladium carbene complexes with a ligand environment that strongly depends on the reaction conditions. Even though we are far from understanding the full details of product selectivity, some relevant factors have been identified including the concentration of the reactants, the wingtip groups of the bisimidazolium ligand, and the presence of an external base. In neutral environment, small wingtip groups (R = Me) give a mixture of monometallic biscarbene complexes and an unprecedented bimetallic A-frame carbene, while larger groups (R = *i*Pr) selectively afford the monometallic species. The presence of a base plays a crucial role during complexation and results in the exclusive formation of tetracarbene complexes. Mechanistic and kinetic analyses of the formation of these tetracarbene complexes revealed that biscarbenes are formed as intermediates. The increased reactivity of the biscarbenes palladium complexes compared to the precursor salt $[Pd(OAc)_2]$ provides further evidence for the high *trans* effect of *N*-heterocyclic carbene ligands. Moreover, this work suggests that palladium salts may produce a range of different products in imidazolium-derived ionic liquid solvents. This is particularly relevant in processes where the formation of the (catalytically) active species occurs in situ.

5. Supplementary material

Crystallographic data (excluding structure factors) for the structures **2b**, **2c**, **3**, **6a** and **6b** have been deposited with the Cambridge Crystallographic Data Centre as supplementary publication nos. CCDC 283149–283153. Copies of the data can be obtained free of charge on application to CCDC, 12 Union Road, Cambridge CB2 1EZ, UK [fax: (int.) +44 1223 336 033; e-mail: deposit@ccdc.cam.ac.uk.

Acknowledgments

We thank F. Fehr and F. Nydegger (University of Fribourg) for technical assistance with NMR and MS measurements, respectively. This work was financially supported by the Swiss National Science Foundation (Grant 200021-101891). M.A. thanks the Alfred Werner Foundation for an Assistant Professorship.

References

[1] (a) T. Welton, Chem. Rev. 99 (1999) 2071;
(b) P. Wasserscheid, W. Keim, Angew. Chem. Int. Ed. 39 (2000) 3772;
(c) J. Dupont, R.T. de Souza, P.A.Z. Suarez, Chem. Rev. 102 (2002) 3667.

[2] (a) T.L. Amyes, S.T. Diver, J.P. Richard, F.M. Rivas, K. Toth, J. Am. Chem. Soc 126 (2004) 4366;
(b) A.M. Magill, K.J. Cavell, B.F. Yates, J. Am. Chem. Soc. 126 (2004) 8717.

[3] (a) A.J. Arduengo, Acc. Chem. Res. 32 (1999) 913;
(b) D. Bourissou, O. Guerret, F.P. Gabbaï, G. Bertrand, Chem. Rev. 100 (2000) 39;
(c) W.A. Herrmann, Angew. Chem. Int. Ed. 41 (2002) 1290.

[4] (a) Other methods include C–H bond activation, oxidative addition, and transmetallation. For representative examples, see S. Gründemann, M. Albrecht, A. Kovacevic, J.W. Faller, R.H. Crabtree, J. Chem. Soc., Dalton Trans. (2002) 2163;
(b) D.S. McGuinness, K.J. Cavell, B.F. Yates, B.W. Skelton, A.H. White, J. Am. Chem. Soc. 123 (2001) 8317;
(c) A. Fürstner, G. Seidel, D. Kremzow, C.W. Lehmann, Organometallics 22 (2003) 907;
(d) H.M.J. Wang, I.J.B. Lin, Organometallics 17 (1998) 972;
(e) A.R. Chianese, X. Li, M.C. Janzen, J.W. Faller, R.H. Crabtree, Organometallics 22 (2003) 1663.

[5] (a) A similar method has been applied for the formation of analoguous pyridinium-derived carbene complexes J.S. Owen, J.A. Labinger, J.E. Bercaw, J. Am. Chem. Soc. 126 (2004) 8247;
(b) M. Albrecht, H. Stoeckli-Evans, Chem. Commun. (2005) 4705.

[6] W.A Herrmann, J. Schwarz, M.G. Gardiner, Organometallics 18 (1999) 4082.

[7] W.A Herrmann, M. Elison, J. Fischer, C. Köcher, G.R.J. Artus, Chem. Eur. J. 2 (1996) 772.

[8] (a) For an example, compare J. Huang, E.D. Stevens, S.P. Nolan, J.L. Petersen, J. Am. Chem. Soc. 121 (1999) 2674;
(b) M. Scholl, T.M. Trnka, J.P. Morgan, R.H. Grubbs, Tetrahedron Lett. 40 (1999) 2247;
(c) T. Weskamp, F.J. Kohl, W. Hieringer, D. Gleich, W.A. Herrmann, Angew. Chem. Int. Ed. 38 (1999) 2416.

[9] (a) For selected references, see U. Kernbach, M. Ramm, P. Luger, W.P. Fehlhammer, Angew. Chem., Int. Ed. Engl. 35 (1996) 310;
(b) R.E. Douthwaite, D. Haussinger, M.L.H. Green, P.J. Silcock, P.T. Gomes, A.M. Martins, A.A. Danopoulos, Organometallics 19 (1999) 4584;
(c) M.V. Baker, B.W. Skelton, A.H. White, C.C. Williams, J. Chem. Soc., Dalton Trans. (2001) 111;
(d) M. Albrecht, J.R. Miecznikowski, A. Samuel, J.W. Faller, R.H. Crabtree, Organometallics 21 (2002) 3596.

[10] R.M. Claramut, J. Elguero, T. Meco, J. Heterocycl. Chem. 20 (1983) 1245.

[11] W.A. Herrmann, C.-P. Reisinger, M. Spiegler, J. Organomet. Chem. 557 (1998) 93.

[12] W.P. Fehlhammer, T. Bliss, U. Kernbach, I. Brüdgam, J. Organomet. Chem. 490 (1995) 149.

[13] W.A. Herrmann, J. Schwarz, M.G. Gardiner, M. Spiegler, J. Organomet. Chem. 575 (1999) 80.

[14] Stoe & Cie, X-Area V1.17 & X-RED32 V1.04 Software, Stoe & Cie GmbH Darmstadt, Germany, 2002.

[15] G.M. Sheldrick, SHELXS-97 Program for Crystal Structure Determination, University of Göttingen, Germany, 1997.

[16] G.M. Sheldrick, SHELXL-97 Program for Crystal Structure Refinement, University of Göttingen, Germany, 1997.

[17] (a) A.L. Spek, PLATON, A Multipurpose Crystallographic Tool, Utrecht University, Utrecht, The Netherlands, 2005;
(b) A.L. Spek, J. Appl. Cryst. 26 (2003) 7.

[18] (a) W.A. Herrmann, M. Elison, J. Fischer, C. Köcher, G.R.J. Artus, Angew. Chem., Int. Ed. Engl. 34 (1995) 2371;
(b) A.A.D. Tulloch, A.A. Danopoulos, G.J. Tizzard, S.J. Coles, M.B. Hursthouse, R.S. Hay-Motherwell, W.B. Motherwell, Chem. Commun. (2001) 1270;
(c) S. Gründemann, M. Albrecht, J.A. Loch, J.W. Faller, R.H. Crabtree, Organometallics 20 (2001) 5485;
(d) J.A. Loch, M. Albrecht, E. Peris, J. Mata, J.W. Faller, R.H. Crabtree, Organometallics 21 (2002) 700.

[19] (a) R.J. Puddephatt, Chem. Soc. Rev. 12 (1983) 99;
(b) F.A. Cotton, G. Wilkinson, C.A. Murillo, M. Bochmann, Advanced Inorganic Chemistry, sixth ed., Wiley–Interscience, New York, 1999, 1039.
[20] M.G. Gardiner, W.A. Herrmann, C.-P. Reisinger, J. Schwarz, M. Spiegler, J. Organomet. Chem. 572 (1999) 239.
[21] X. Creary, E.A. Burtch, Z. Jiang, J. Org. Chem. 68 (2003) 1117.
[22] (a) N. Kornblum, J.W. Powers, G.J. Anderson, W.J. Jones, H.O. Larson, W.M. Weaver, J. Am. Chem. Soc. 79 (1957) 6562;
(b) N. Kornblum, W.J. Jones, G.J. Anderson, J. Am. Chem. Soc. 81 (1959) 4113.
[23] T. Steiner, Cryst. Rev. 6 (1996) 1.